

Optical low-coherence reflectometry characterization of cladding modes excited by long-period fiber gratings

D. Varelas, A. Iocco, H. G. Limberger, and R. P. Salathé

Institute of Applied Optics, Swiss Federal Institute of Technology, CH-1015 Lausanne, Switzerland

S. A. Vasiliev, E. M. Dianov, O. I. Medvedkov, and V. N. Protopopov

Fiber Optics Research Center, General Physics Institute of the Russian Academy of Sciences, 38, Vavilov Street, 117756 Moscow, Russia

Received June 7, 1999

The group refractive-index difference of cladding modes excited by a long-period fiber grating is characterized by use of the technique of optical low-coherence reflectometry, with a precision of $<10^{-4}$. Very good agreement between theoretical and experimental results is demonstrated. © 1999 Optical Society of America
 OCIS codes: 050.2770, 120.1840, 290.3030, 030.4070, 060.2270.

In-fiber gratings are widely used for many important applications in telecommunication and sensor systems. In both Bragg and long-period gratings cladding-mode coupling is present. Despite their importance, cladding modes excited by gratings have not been well investigated. In this Letter we propose a new quantitative method to measure the group index of the cladding modes excited by long-period gratings as well as the cladding-mode propagation behavior along the fiber. The proposed technique is based on the application of optical low-coherence reflectometry (OLCR), which is typically used to characterize integrated optical components.¹ Recently, Salathé *et al.* showed that the OLCR technique allows one to measure the group index of modes and to investigate the intermodal coupling in a multicore fiber.² To obtain these parameters they analyzed the OLCR signal of the Fresnel reflection from the end of the fiber that was tested. The same approach is used here for the investigation of the properties of pure cladding modes excited by long-period gratings.

For the OLCR measurements a commercial reflectometer (Hewlett-Packard HP 8504B) was used. To analyze the group indices of the cladding modes we connected the fiber that contains the long-period grating to the measuring arm of the reflectometer (Fig. 1). We carefully stripped off the polymer coating and cleaned the fiber length after the grating to avoid cladding-mode dissipation in the coating. Potential effects of the coating, if it is not fully removed, or of different media that could come into contact with the fiber will require additional investigations, which were not carried out in our experiments. Two different LED sources operate in the reflectometer, with peak wavelengths at 1.31 and 1.55 μm , respectively. The optical bandwidth (FWHM) of both LED sources is ~ 55 nm, which corresponds to FWHM coherence lengths in the fiber of 17 and 50 μm at 1.3 and 1.55 μm , respectively. We chose the grating parameters to place one resonant cladding-mode peak in each LED wavelength range. The LED light propagates all the way to the cleaved fiber end, where it is partially backreflected. Observation of a reflected signal is possible under the

condition that the optical path-length difference between the reference arm and the measurement arm is smaller than the coherence length of the light source. The optical path length of the detected signal, which is defined as the round trip to the fiber end and back, depends on the group index of the modes in which light propagates and is different for the fundamental and the cladding modes, as they have different group indices. Signal intensity is defined by the energy dissipation of each mode (owing to intermodal coupling, absorption or radiation losses, etc.) and by the quality of the fiber end.

In our experiments long-period gratings were written in a single-mode germanosilicate fiber. The fiber had a step-index profile with a core/cladding index difference of 0.017 and core and cladding diameters of 3.4 and 125 μm , respectively. Gratings were fabricated by a step-by-step technique by use of a cw frequency-doubled Ar^+ laser³ ($\lambda = 244$ nm) and the following irradiation conditions: UV intensity $I = 20$ kW/cm^2 , accumulated UV dose $D = 20$ kJ/cm^2 . The period and the length of the gratings were 162 μm and 20 mm, respectively. In this case the HE_{17} and the HE_{10} modes were placed in the output spectra of the 1.31- and the 1.55- μm LED sources, respectively. The gratings were characterized by use of a halogen lamp and a monochromator with a typical resolution of 1 nm. Several similar gratings were prepared and used for the OLCR experiments. Their typical parameters were as follows: For the peak related to HE_{11} and HE_{17} mode coupling the resonance wavelength, the coupling, and the FWHM were approximately 1.32 μm , 3 dB, and 6.5 nm, respectively. The same parameters for HE_{11} and HE_{10} mode coupling were approximately 1.55 μm , 10 dB, and 8.5 nm, respectively.

The group indices of the fundamental and the HE_{1m} ($m = 2-11$) cladding modes calculated for the fiber used are shown as a function of wavelength in Fig. 2. We performed the calculation by solving the wave equations numerically to obtain the effective refractive index n_{eff} of each mode.³ The group index n_{gr} was then obtained by use of the following relation: $n_{\text{gr}} = c/v_{\text{gr}} = n_{\text{eff}} - \lambda(dn_{\text{eff}}/d\lambda)$, where c is

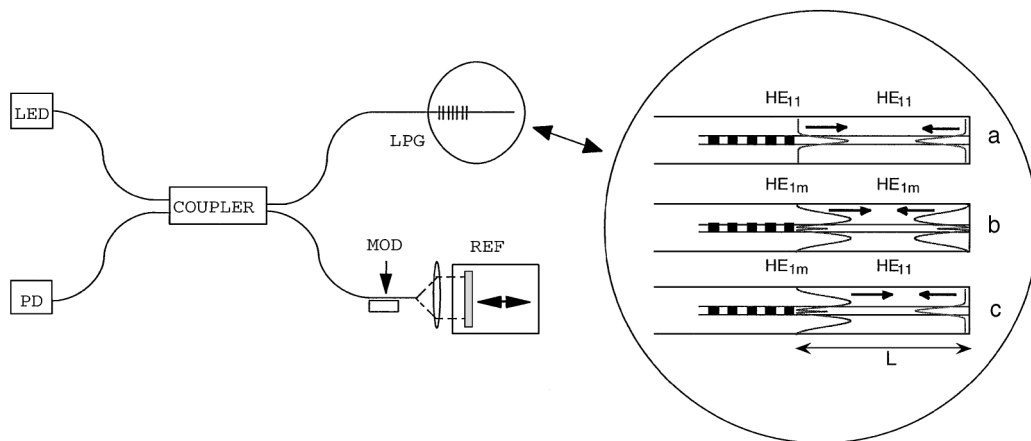


Fig. 1. Scheme of the OLCR measurement setup: PD, photodiode; LPG, long-period grating; MOD, modulator; REF, reference mirror. The inset shows the mode-propagation scheme.

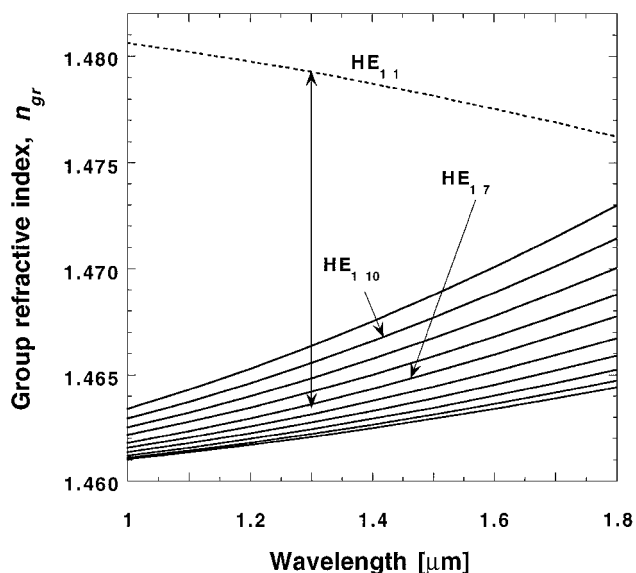


Fig. 2. Calculated group indices of core (HE_{11}) and cladding modes (HE_{1m}).

the light velocity in vacuum, v_{gr} is the mode group velocity, and λ is the wavelength.

Figure 3 presents the OLCR signal as function of the OLCR delay with respect to the fundamental mode [peak (a)] for the 1.55- μm LED source. We obtained the spectra shown in Fig. 3 by cutting different fiber lengths after the grating. For better presentation the intensities of successive spectra for different fiber lengths were shifted upward by constant values, which are indicated on the right-hand side of each spectrum. The remaining distance L from the grating to the fiber end is shown on the left-hand side of each spectrum. Three peaks were observed in our measurements. The strongest peak, peak (a), corresponds to the fundamental mode HE_{11} , which is reflected by the fiber end to the backward-propagating fundamental mode (see diagram a in the inset of Fig. 1). Peak (b) is due to cladding mode HE_{110} , which is excited by the grating and is backreflected at the fiber end to the same cladding mode (diagram b in the inset of Fig. 1). Then this mode is partially coupled back by the grating to the fundamental mode and detected by a

photodiode. The top line with the arrows in Fig. 3 indicates the optical distance between the fundamental-mode peak (a) and the cladding-mode peak (b), which is equal to the group-index difference between these modes, Δn_{gr} , multiplied by $2L$. Peak (c) corresponds to the partial coupling of cladding mode HE_{110} to fundamental mode HE_{11} and vice versa, which takes place at the fiber end (diagram c in the inset of Fig. 1). In this case the optical distance between peaks (a) and (c) is given by Δn_{gr} multiplied by L . The FWHM of the HE_{11} peaks is wider than the OLCR accuracy owing to the fiber dispersion difference between the reference and the measurement arms, which was ~ 20 ps/(nm km). The same measurement was performed at 1.31 μm for the HE_{17} cladding mode. Figure 4 presents the absolute value of the OLCR delay between the cladding and the fundamental modes as a function of L . The squares and circles correspond to the measured HE_{17} and HE_{110} modes, respectively.

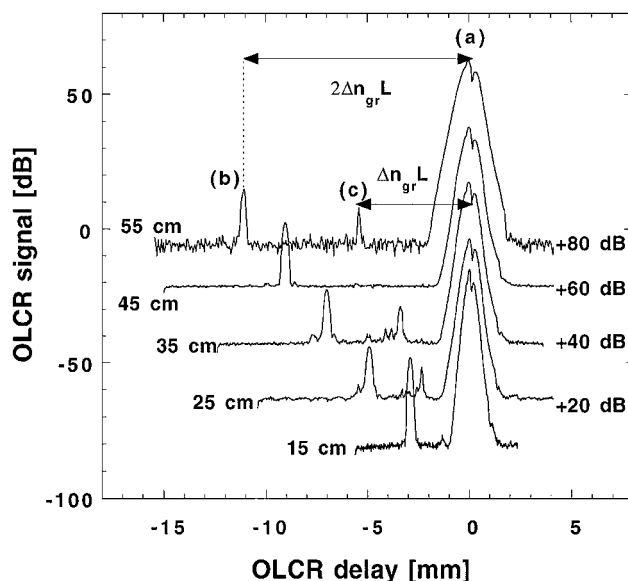
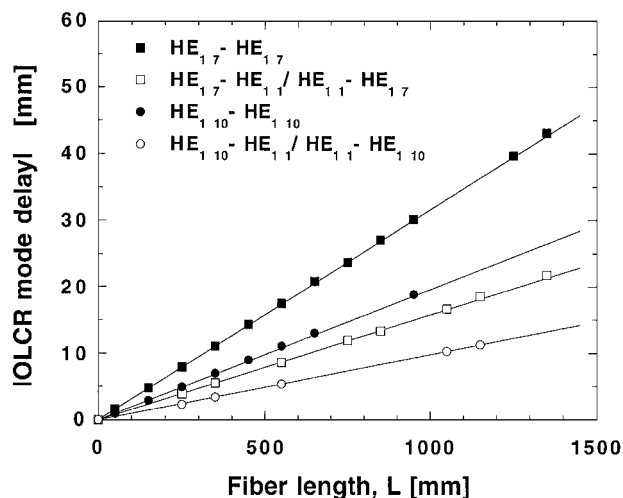


Fig. 3. OLCR signal of (a) the fundamental mode and (b), (c) cladding mode HE_{110} for different fiber lengths at 1.55 μm .

Table 1. Theoretical and OLCR Experimental Data of Cladding Modes Excited by Long-Period Gratings

Experimental Data	Mode Coupling			
	HE ₁₇ -HE ₁₇	HE ₁₇ -HE ₁₁ /HE ₁₁ -HE ₁₇	HE ₁₁₀ -HE ₁₁₀	HE ₁₁₀ -HE ₁₁ /HE ₁₁ -HE ₁₁₀
Peak wavelength (μm)	1.31	1.31	1.55	1.55
Δn_{gr}				
Measured	0.0158 ± 0.0001	0.0079 ± 0.0001	0.0098 ± 0.0001	0.0049 ± 0.0001
Calculated	0.0156	0.0078	0.0095	0.0048

Fig. 4. Absolute value of OLCR delay versus fiber length for the HE₁₇ and the HE₁₁₀ cladding modes.

The OLCR delays of the different cladding modes with respect to the fundamental mode are proportional to the fiber length L . The slopes of the curves that correspond to the coupling between cladding modes [peak (b) in Fig. 3] are equal to $2\Delta n_{\text{gr}}$. In contrast, the slope of the curve that corresponds to the cross coupling between the fundamental and the cladding modes at the fiber end [peak (c) in Fig. 3] is equal to Δn_{gr} . The slopes of the solid lines in Fig. 4 are based on theoretical calculation of Δn_{gr} between the fundamental and the cladding modes, which is illustrated in Fig. 2. All experimental and calculated values are given in Table 1. Very good agreement of the experimental results with calculations can be observed. The fact

that the slope of peak (c) is exactly half the slope of peak (b) confirms the previous argument on the origin of peak (c). The errors, which are indicated in Table 1, are essentially given by the precision in measuring the length between the grating and the fiber end. Increasing the propagation length could further decrease the actual error, which is in the worst case 10^{-4} .

In conclusion, the OLCR method has been applied to measure the group-index difference of cladding modes excited by long-period gratings with an accuracy of better than 10^{-4} . Very good agreement with theoretical calculations has been observed.

This work was realized within the framework of an institutional partnership between the Institute of Applied Optics-Swiss Federal Institute of Technology and the Fiber Optics Research Center-General Physics Institute, which was sponsored by the Swiss National Science Foundation. Partial sponsorship by the European Advanced Communications Technologies and Services (ACTS) Project is also acknowledged. H. G. Limberger's e-mail address is hans.limberger@epfl.ch.

References

1. P. Lambelet, P. Y. Fonjallaz, H. G. Limberger, R. P. Salathé, C. Zimmer, and H. H. Gilgen, *IEEE Photon. Technol. Lett.* **5**, 565 (1993).
2. R. P. Salathé, H. Gilgen, and G. Bodmer, *Opt. Lett.* **21**, 1006 (1996).
3. S. A. Vasiliev, E. M. Dianov, A. S. Kurkov, O. I. Medvedkov, and V. N. Protopopov, *Quantum Electron.* **27**, 146 (1997).